COMBUSTION ASPECTS OF ALCOHOL SPRAY COMBUSTION WITH THE PRESENCE OF AN ACOUSTIC FIELD

Alexandre Dias Flügel, flugel@ita.br
Pedro Teixeira Lacava, placava@ita.br
Instituto Tecnológico de Aeronáutica, Pça.Mal. Eduardo Gomes, n°50, São José dos Campos - SP, 12228-900

Ely Vieira Cortez, evcortez@lcp.inpe.br
Marco Aurélio Ferreira, marco@lcp.inpe.br
Instituto Nacional de Pesquisas Espaciais, Rodv. Presidenre Dutra, km 40, Cachoeira Paulista - SP, 12630-000

João Andrade de Carvalho Júnior, joao@feg.unesp.br
Universidade Estadual Paulista, Av. Dr. Ariberto Pereira da Cunha, n°333, Guaratinguetá - SP, 12500-000

Abstract. *The present work shows the experimental results for ethanol spray combustion with air in different equivalence ratios and acoustic oscillation. The experiments were conducted in a vertical laboratorial scale combustion chamber with water jacket for refrigeration. For fuel atomization a pressure swirl atomizer was used and the acoustic excitation was done using a speaker strategically positioned in the air combustion feed line. The results show the acoustic excitation change strongly the emissions of unburned hydrocarbons, carbon monoxide, and nitrogen oxides. Basically the experiments show that the displacement fluctuation on the combustion air flow, due to the presence of the acoustic field, has strong influence in the combustion. The NO_x emission initially increases with the acoustic field presence; but when the maximum acoustic velocity overcomes de average flow velocity, the NO_x emission reduces. Therefore, the spray pulsed combustion is a promissory technology to conciliate NO_x emissions with partial oxidation pollutants.*

Keywords*: pulsating combustion, pulsed burners, acoustic displacement, combustion with acoustic actuation, pollutant emissions.*

1. INTRODUCTION

The pulsating combustion process has been object of important research due to the potential that its application on energy generation may offer several advantages, such as: fuel savings, lower partially oxidized pollutant formation, and increased convective heat transfer (Zinn, 1996). Pulsating combustion can be considered as a combustion process in which the state parameters are submitted to oscillatory conditions; therefore, they change periodically with time (Zinn, 1986). In conventional combustion processes there are no correlations between the fluctuations established in a determined point of combustion chamber and the fluctuations established in another point (Libby and Williams, 1994). However, for pulsating flames, the temporal or special correlations are organized and higher amplitudes are reached.

Yoshida et al. (2001) have studied the presence of an acoustic field in turbulent jet diffusion flames, and they observed that at the resonant conditions the transient from laminar to turbulent flow is enhanced, and consequently the turbulent intensity of the flow increases markedly. But the long predominantly diffusive flames are normally not able to auto-excite acoustically the confined combustion, neither to amplify the oscillations in the case of external actuation, as presented by Ferreira et al. (2006). When the acoustic oscillation is applied to an originally diffusion flame, the traditional aspect of this kind of flame changes to look like a predominant premixed flame, with large quantities of oxygen into the jet fuel side (Rocha et al., 2006).

The knowledge about those processes is fundamentally important because the pulsating combustion technology has demonstrated a potential to lower pollutant emissions. The pulsations intensify the mixing rate between the reactants; therefore, the combustion process is more intense, with lower amounts of fuel wasted, and low partial oxidation pollutants, as CO and soot. However, there are no sufficient researches to investigate completely the nitrogen chemistry and the NO_x formation in pulsating flames. NO_x is the result of the complex interaction between the fluid dynamics and the chemistry. During the combustion phase of the cycle, significant space and temporal gradients of temperature occur in the combustor; due to the mechanism of heat transfer is not fast enough to maintain the temperature homogeneous. Locally the temperature can approach the adiabatic flame temperature and the gradients can be higher than 300K, favoring NO_x formation (Glarborg, 1993). In general the mixture controls those gradients, and they occur more pronouncedly in non-premixed systems (Keller et al., 1993). In this way, the great challenge of the pulsating devices is to adjust the emissions of partial oxidation pollutants and the NO_x emission.

The present paper is concerned about the influence of the acoustic field in the combustion of spray, mainly in the aspect of NO_x, carbon monoxide, and unburned hydrocarbons (UHC) emissions. The objective is to relate the oscillation conditions, not only the frequency and the amplitude, but also the flow displacement, with the emissions of the cited pollutants.

The liquid fuel injection process plays an important role in many aspects of combustion processes performance. To obtain the surface to mass high ratios in the liquid phase which lead to the desired very high evaporation rates, the liquid fuel must be fully atomized before being injected into the combustion zone. The oscillations can affect the spray characteristics, especially the droplet size distribution. Dubey et al. (1997) have studied the spray combustion into a Rijke tube pulsating combustion operating with 80 Hz and 155 db. Using a phase Doppler particle size diagnostic system the authors investigated the spray Sauter Mean Diameter (SMD) for pulsating and non-pulsating combustion. They concluded that the SMD mean reduction was 15% for the pulsating situation in compared to non-pulsating.

Dattaraja et al. (2006) recently studied the methanol droplets combustion submitted to oscillation in a gravity and microgravity environment. The study was conducted firstly in the pressure nodes, where the acoustic velocity is higher, and after at the pressure antinodes, where the acoustic pressure is higher. The acoustic excitation had better results for microgravity. In normal gravity the combustion rate increase up to 15% in the nodes; however, no significant changes were observed for the antinodes. For the microgravity the combustion rate increases were 75% and 200% for the antinodes and nodes region, respectively.

Atomization is usually accomplished by spreading the fuel into a thin sheet to induce instability thus promoting its disintegration into ligaments which collapse into droplets due to surface tension action. The discharging of the fuel through orifices with specially shaped passages, leads the fuel to become a thin sheet from which ligaments and ultimately droplets are formed, and these resulting droplets will be distributed through the combustion zone in a controlled pattern and direction.

The fuel thin sheet spread in pulsed gas flow will enhance the ligaments disintegration anticipating the droplets formation and reducing the droplets size. Of course this new scenario will change the spray combustion. For example, the D^2 law (D is the droplet diameter) is also valid for droplet combustion in an acoustic field, and the difference with the acoustic process is the enhancement of diffusion, which increases the combustion constant and consequently reduces the overall burning time of the droplet. In addition, the pulsed flow intensifies the mixing process of vaporized fuel with surrounding air; therefore, the expectative is a more homogeneous combustion for the gas phase, which is very good situation to reduce the partial oxidation pollutants; however, for NO_x it will depend of the overall combustion equivalence ratio.

2. EXPERIMENTAL SETUP

The Figure 1 presents a schematic diagram of the experimental setup used in the present work. The combustor is 1.25 m long, has an internal diameter of 0.25 m, and a decoupling chamber is mounted at its top. This chamber allows continuous analyses of the combustion gases without the interference of the external ambient air; at the same time, it assures the required open end acoustic boundary condition at the combustor exit section. Water-cooled walls were used to control the operating temperature of the reactor walls.

The speaker for acoustic actuation was fed by a sinusoidal signal, generated by Aligent 33120A function generator, and amplified by Proximity-750AP 480 W amplifier. The speaker power was 450 W_{RMS} and the impedance was 8 Ohms.

Kistler 7261 piezoelectric transducers monitored the acoustic pressure in the chamber at 0.0, 0.50 and 0.75 m from the combustor base (P2, P3 and P4, respectively). The pressure signals were amplified by Kistler 5006 charge amplifiers and monitored by a Tektronix 7633 oscilloscope. Average gas temperatures were measured with chromel-alumel thermocouples placed at 0.10, 0.25, 0.50 and 0.75 m from the combustor base (T1, T2, T3 and T4, respectively).

The combustion gases were collected in the combustor exit by water refrigerated probe. The vacuum pump sampled the gases, which flowed through the condensers and filters, to remove the liquid water and particulate material before reaching the continuous gas analyzers (infra-red for CO and CO_2, thermo-magnetic for O_2, chemiluminescent for NO, and polarized electrode for unburned hydrocarbons).

The combustion air mass flow rate was measured with orifice plate and the fuel by a turbine flow-meter. The alcohol mass flow rate was set at 1.25 g/s for all experiment, and the air depends on the global equivalence ratio (0.59 to 0.94), defined as:

$$F = \frac{[m_{air}/m_f]_{st}}{[m_{air}/m_f]_{exp}} , \tag{1}$$

where m_{air} and m_f are the combustion air and fuel mass flow rates, and the subscripts st and exp are referent to stoichiometry combustion and experimental condition, respectively.

All the data were collected and reduced by a computerized data acquisition system (National Instruments AT-MIO 16E1). The system was configured to record at a rate of 6 per minute; each value corresponded to the average of twenty temperature data, one hundred acoustic pressure data, and fifty gases analysis data. All data presented in this work were averages of at least five minutes of acquisition.

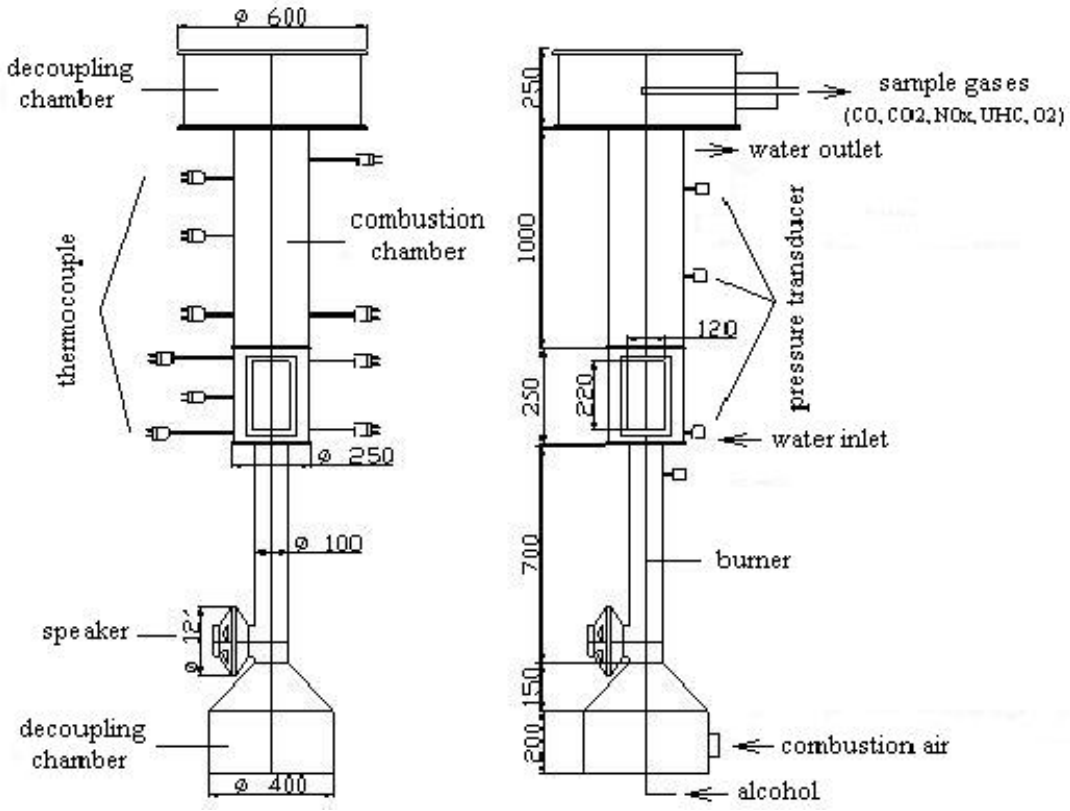

Figure1. Schematic diagram of the experimental setup (dimensions in cm).

The acoustic excitation was done by the speaker strategically positioned in burner air flow duct. The burner was designed to have an acoustic behavior of both-sides opened tube, which means a ½ wave tube. The air duct has 700 mm of length and 3" of diameter, and a chamber was positioned in the air inlet side, where the air was introduced. The Figure 1 also shows the burner scheme and the piezoelectric pressure transducers positions to identify the harmonic frequencies (positions of pressure nodes).

The Figure 2 presents the acoustic responses for excitation range from 50 Hz to 1300 Hz (steps to 5 Hz) for the burner decoupled of the combustion chamber. The results for predominant frequencies are in accord to the theoretical predictions for both-sides opened tube. Based on the diagram, two frequencies were chosen for the combustion studies, 264 Hz and 750 Hz, and the reasons are their acoustic displacement behaviors, commented in the next section.

Without combustion, the spectrum of frequency presented in Figure 2 is also observed in the burner duct when it is coupled to combustion chamber. However, the chamber dumps the oscillation outside the burner. Just to resume the results, when the speaker was fed with 10V and 264 Hz, the maximum acoustic pressure in the duct (transducer positioned at L/2, in this case) is close to 3 kPa, and the acoustic pressure in the chamber at 0.0, 0.50 and 0.75 m from the combustor base were 0.2, 0.17, an 0.3 kPa, respectively. With combustion, the dumper effect increased, for the same excitation condition the responses for 0.0, 0.50 and 0.75 m from the combustor base were 0.1, 0.13, and 0.05 kPa, respectively. The same tendency was observed for 10V and 750 Hz. These results show that the oscillation amplitudes in the combustor did not reach 10% of the amplitude induced by the speaker on the combustion air flow. Therefore, for the present experiments, it can be assumed that the modifications in the flame structure are consequence of acoustic actuation in the burner air flow, and the weak oscillation in the combustor produces minor effects.

It was also observed experimentally that the presences of decoupling chambers in the burner inlet and in the combustion chamber exit did not change the acoustic behavior in both devices.

For the alcohol spray combustion a pressure swirl injector was utilized to atomizes the liquid. The liquid is fed to the injector through four tangential passages giving the liquid a high angular velocity, and forming, in the swirling chamber, a liquid layer with a free internal surface, thus creating a gas-core vortex. The liquid then is discharged from the nozzle in the form of a hollow conical sheet which breaks up into small droplets. The methodology proposed by Lacava et al. (2004) was used to design the injector.

Concentrically to the injector, a flame-holder disc was positioned to maintain the flame close to the burner, especially important in the case with acoustic oscillation. The flame-holder has external diameter of 50 mm and 24 holes of 2 mm distributed in a diameter of 30 mm.

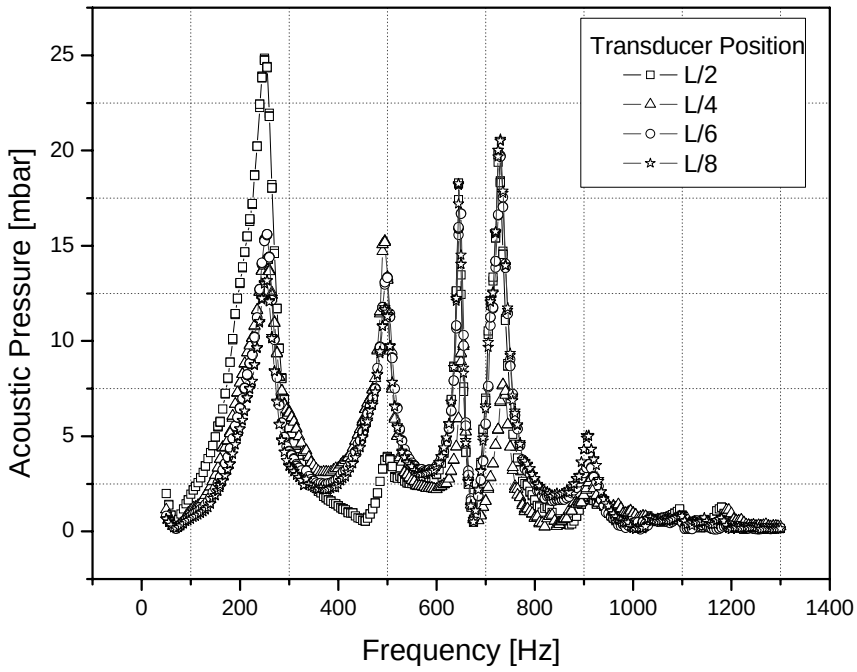

Figure 2. Spectrum of frequency into the burner duct.

3. THE BURNER ACOUSTIC CHARACTERISTICS

The experimental parameters that define the situation of acoustic excitation are the frequency and the amplitude. However, the parameter that is really important to change the combustion structure is the acoustic displacement when the flow emerges from the burner. The acoustic displacement is important to identify the flow acceleration or deceleration and the inversion of direction. Basically the displacement indicates qualitatively the tendency of the air flow movement in the spray combustion zone, which is important to the fuel vapor and the air mixing process, and it can be calculated solving the acoustic equations.

The Equations 2 and 3 are the acoustic pressure (p') and the acoustic velocity (u') equations derived from the linear momentum equation and energy equation. To solve them, the origin of the time (t) is attributed such that acoustic pressure (p') agrees with sin (ωt); where ω is the angular frequency. General solutions for the pressure and acoustic velocity equations can be found using the separation of variables method.

$$\frac{\partial^2 p'}{\partial t^2} - c^2 \frac{\partial^2 p'}{\partial x^2} = 0 \tag{2}$$

$$\frac{\partial^2 u'}{\partial t^2} - c^2 \frac{\partial^2 u'}{\partial x^2} = 0 \tag{3}$$

The sound velocity c is calculated for the average value of temperature. The equations (4) and (5) represent the solution of these equations:

$$p' = c\overline{\rho}\left(A \sin\frac{\omega x}{c} - B\cos\frac{\omega x}{c} \right)\sin\omega t \tag{4}$$

$$u' = \left(A \sin\frac{\omega x}{c} + B\cos\frac{\omega x}{c} \right)\cos\omega t \tag{5}$$

The average density $\overline{\rho}$ is obtained by the ideal gas equation for average values of pressure and temperature, and A and B are constants. For a both-sides opened tube with length of L, the boundary conditions are:

$$p' = (0,t) = 0 \tag{6}$$

$$p' = (L,t) = 0 \tag{7}$$

To satisfy the boundary condition (6) in the analytical solution equation (3), B must be zero; and applying the boundary condition (7) in the equation (3), the result for ω is:

$$\omega = \frac{nc\pi}{L} \tag{8}$$

Therefore, the result for the pressure acoustic for both-sides opened tube is:

$$p' = c\bar{\rho}A \sin\frac{nx\pi}{L} \sin\frac{n\pi ct}{L} \tag{9}$$

For the acoustic velocity the result is:

$$u' = A \cos\frac{nx\pi}{L} \cos\frac{n\pi ct}{L} \tag{10}$$

The relation between $p`_{max}$ and $u`_{max}$ is (maximum acoustic pressure and acoustic velocity):

$$p'_{\max} = Ac\bar{\rho}\text{, and } u'_{\max} = A\text{; so: } u'_{\max} = \frac{p'_{\max}}{c\bar{\rho}} \tag{11}$$

Therefore, the acoustic displacement η' is calculated through of the acoustic velocity integral, equation (10):

$$\eta' = \int_0^t A \cos\frac{nx\pi}{L} \cos\omega t \, dt = \frac{u'_{\max}}{\omega}\frac{\cos nx\pi}{L}.\sin(\omega.t) + k \tag{12}$$

The constant k physically represents the initial position (x_0). For the maximum acoustic displacement, the oscillatory part tends to one and the solution is:

$$\eta'_{\max} = \frac{A}{\omega} = \frac{A}{2\pi f} = \frac{AL}{nc\pi} = \frac{u'_{\max}}{\omega} \tag{13}$$

The acoustic displacement is an important parameter to identify the behavior of the pulsed flow, because it depends on the frequency of excitation, acoustic pressure, average temperature and pressure, sound velocity, and the acoustic characteristic of the burner (in the present case both-sides opened tube). Therefore, in spite of the frequency and amplitude of excitation in the speaker, the changes in the emissions must be analyzed comparing with the total displacement, which is the natural flow displacement (the same without oscillation) plus the acoustic displacement. For the case $x = x_0 = 0$, the total flow displacement is:

$$\eta_t = u.t + \eta_{\max}.\sin(w.t) \tag{14}$$

Some calculations were done for typical experimental situations, which means $\bar{\rho}$ = 1.001 kg.m^{-3} and c = 365 m.s^{-1}. The combustion air average velocity (u) in the burner was calculated using the mass conservation equation for different values of equivalence ratio F. For experimental frequencies and equivalence ratios, values of p'_{max} were arbitrated, and u'_{max} was calculated by equation (11). These calculations are resumed in the Figure 3 that presents the u'_{max}/u ratio versus p'_{max}.

The Figure 3 shows that the u'_{max}/u ratio increases when the acoustic pressure also increases. The acoustic velocity tends to overcome the average flow velocity, and the change happens in the range from 1.5 kPa to 2.0 kPa for all cases simulated. Experimentally, modifications in the emissions tendency were observed in this range, and they are presented and commented in the next section. In addition, also experimentally it was possible visualize the flame-holder red

incandescence when theoretically u'_{max} overcame u, which is an indication of the intense combustion close to spray injector.

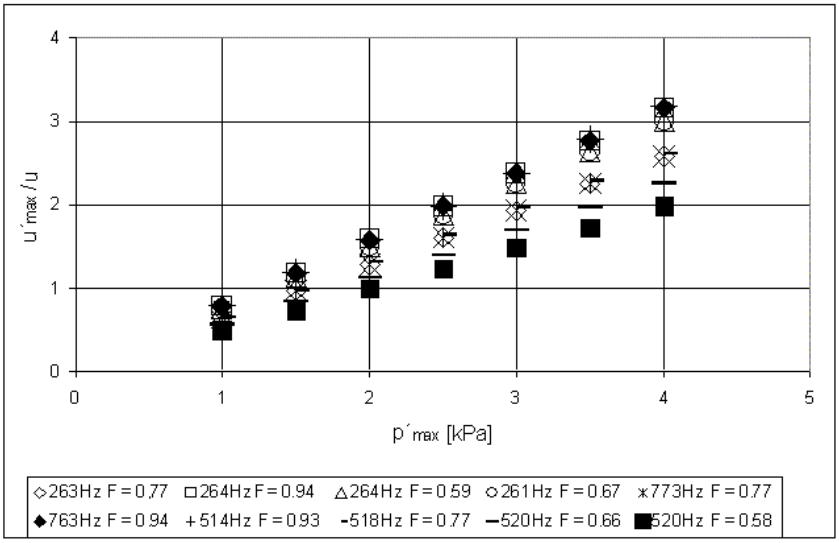

Figure 3. Ratio u'_{max}/u versus p'_{max} for different global equivalence ratios (F) and frequencies.

The Figure 4 shows the total flow displacement calculated by equation (14) for a typical experimental value u = 3 m/s, frequencies of 264 Hz and 750 Hz, and the arbitrary values for p'_{max} , 1.5 kPa and 3.5 kPa. The graphics show that the displacement fluctuation increases when acoustic pressure also increases, but reduces with the frequency. For 264 Hz and 1.5 kPa, the flow has successive decelerations and accelerations; and when the p'_{max} is 3.5 kPa the flow has successive inversions of direction. However, the fluctuations suffer attenuation when the frequency becomes 750 Hz.

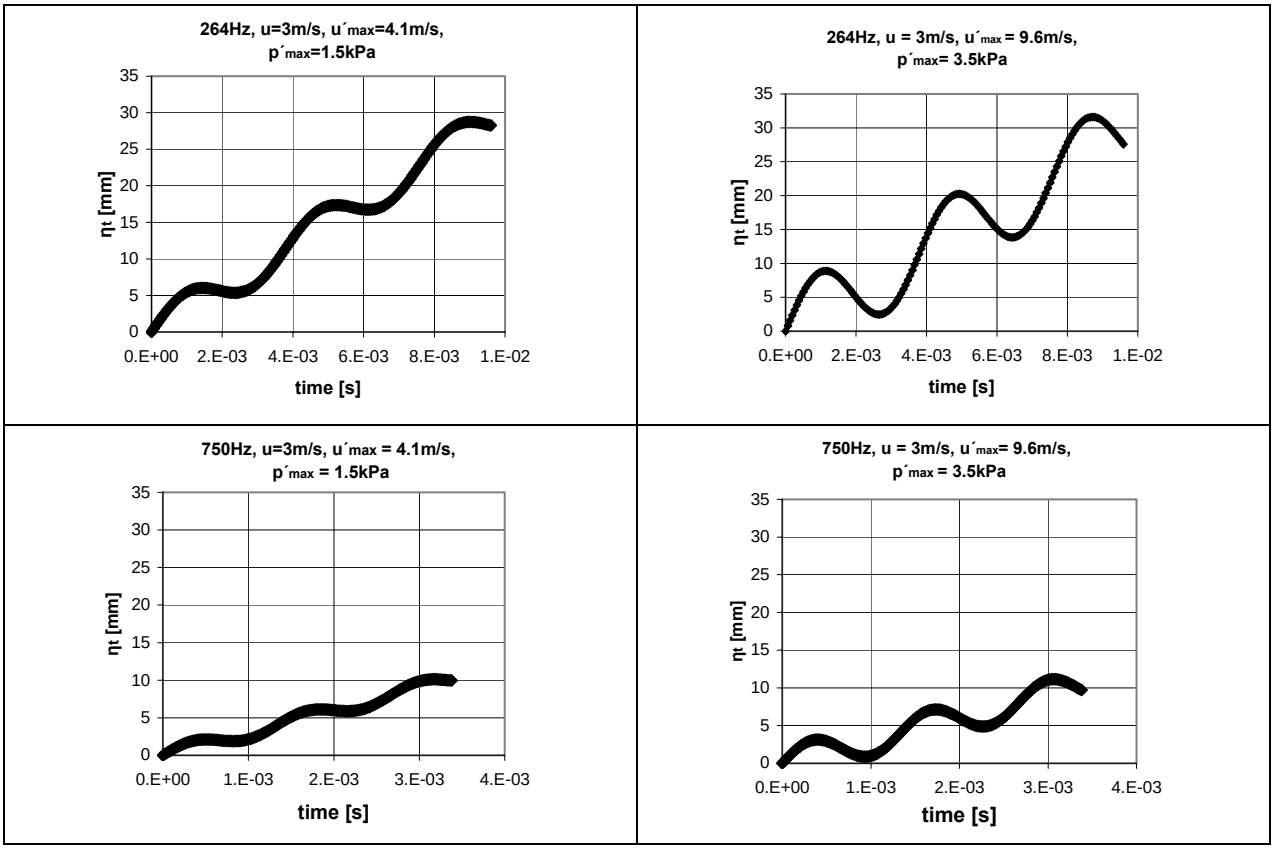

Figure 4 - Total displacement for different excitation conditions.

Extrapolating this behavior to the flame region, this air flow oscillatory movement will probably intensify the air entrainment into the spray flame region. In addition, as commented in the introduction, the presence of the oscillations reduces the droplet vaporization time. Therefore, because the combination of these two effects, the expectative is an intense mixing process between the combustion air and fuel vapor.

To compare and verify the influence of the displacement fluctuation in the spray pulsating combustion, the results for frequencies 264 Hz and 750 Hz are presented in the next section.

4. RESULTS FOR GAS ANALYSES

The Figures 5, 6, 7 show the emissions of NO_x, CO and UHC, respectively, versus de maximum acoustic pressure in the burner duct, for 264 Hz and different global equivalence ratios. The emissions were corrected to 3% of O_2 in the combustion gases and are in dry base.

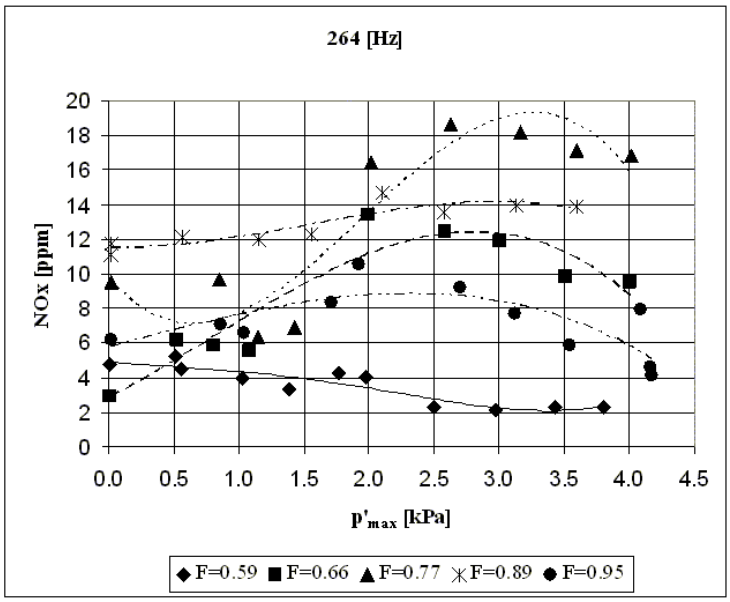

Figure 5. NO_x emission versus p'_{max} , for 264 Hz and several equivalence ratios (F).

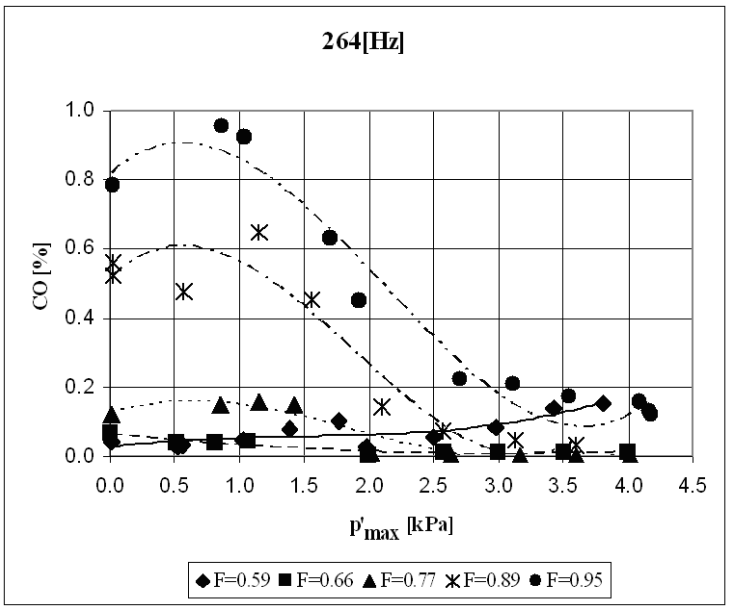

Figure 6. CO emission versus p'_{max} , for 264 Hz and several equivalence ratios (F).

The present experiment was conduct in a refrigerated chamber; therefore, the maximum temperature in the exhaust gases was 1000 K, and the expectative of low emissions of NO_x and high emissions of CO and UHC were confirmed experimentally.

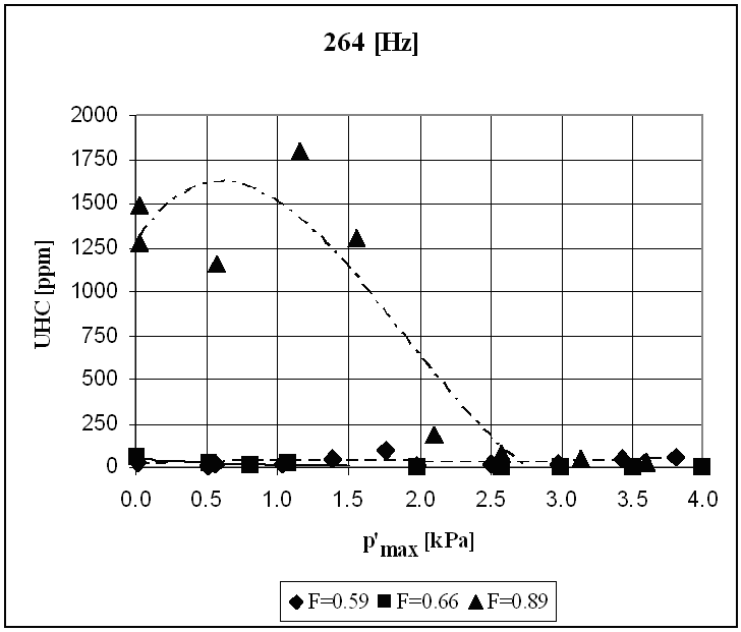

Figure 7. UHC emission versus p'_{max} , for 264 Hz and several equivalence ratios (F).

Without acoustic oscillation the higher NO_x emission are displaced from stoichiometry to the lean side of combustion, more specifically, to the equivalence ratios of 0.89 and 0.77. For leaner global equivalence ratio the emission decreases.

Except in the case of F = 0.59, in the other ones equivalence ratio there is an average initial tendency of NO_x increase; however, after $p`_{max}$ 1.5 or 2.0 the tendency is reduction. Take into account that the pulsed flow intensifies the mixing process between fuel vapor and the air, and accelerates the droplets vaporization, changes observed in other works for pulsed flow in gas fuel combustion can be used to explain the present behavior. Taking as example the work of Rocha el al. (2006) for Delft pulsed natural gas jet diffusion flames, it shows that increasing the acoustic pressure the quantity of air entraining in the fuel side of the jet also increases. Therefore, the original diffusion flame becomes a partial pre-mixed flame with the intensification of the acoustic pressure. For the present situation, the initial application of p'_{max} lower than 1.5, probably carries more oxygen to mix with the fuel vapor, the temperature in flame region increases, and, consequently, the NO_x emission also increases. But, when the p'_{max} reaches values superior than 1.5 or 2.0, the maximum acoustic velocity overcomes the average flow velocity (as presented in the anterior section), intensifying the air entrainment, and, probably, creating a lean pre-mixed combustion, reducing the temperature and NO_x emission. For the case of F = 0.59, the large excess of air did not allow the increase of temperature, and every increase of acoustic pressure reduced the NO_x emission.

For the CO emissions, the inverse behavior of NO_x is observed, enhancing the acoustic pressure the CO emission reduces as consequence of the pre-mixed effect. Just for F = 0.59 this tendency is not observed, and the CO emissions increases with p'_{max}. In this case, following the same reasoning for NO_x, more air entrainment turns down the temperature and the CO to CO_2 conversion mechanism becomes slower.

The Figure 7 shows that for F = 0.89 the behavior of UHC with respect to presence of acoustic excitation is the same of CO. For F = 0.67 and 0.59 small quantities of UHC is present and the acoustic field has little influence.

Based on the comments of the anterior section, for the frequency of 264 Hz the flow displacement fluctuation is intense and increases with acoustic pressure. This fluctuation has a primordial influence in the air entrainment, and, as consequence, in the combustion structure. To compare, the Figures 8, 9, and 10, show the NO_x, CO, and UHC emissions, respectively, for 750 Hz, where the flow displacement fluctuation is not intense. The complete verification was done just for F = 0.94 and 0.77, but for the others global equivalence ratio some specifics texts were conducted and the same tendency was observed, which means the presence of the acoustic field was minor importance. No significant change happened in the emissions when the acoustic pressure increases, due to the low displacement fluctuation.

Comparing the Figures 5 and 8, some variations for NO_x are observed for the non-excitation conditions, which are results for testes executed in different days; but variations are close to the analyzer sensibility.

5. CONCLUSIONS

The present work investigated the NO_x, CO and UHC emissions in the alcohol spray combustion with the presence of an acoustic field. The results showed that the most important acoustic parameter to change the spray flame structure and control the combustion process is the fluctuation of the flow displacement. Of course this fluctuation is consequence of the excitation frequency and amplitude; however, the solution of acoustic equations showed that the

displacement increases with the acoustic pressure and decreases with frequency. Therefore, the excite parameters must be combined to introduce in the flame region fluctuations on the flow displacement able to modify the flame dynamic.

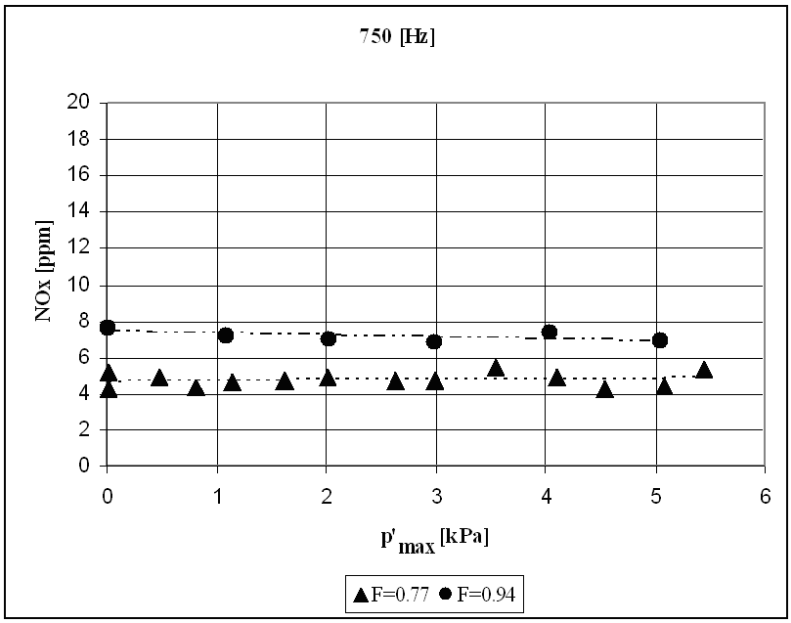

Figure 8. NO_x emission versus p'_{max} , for 750 Hz and equivalence ratios (F) of 0.77 and 0.94.

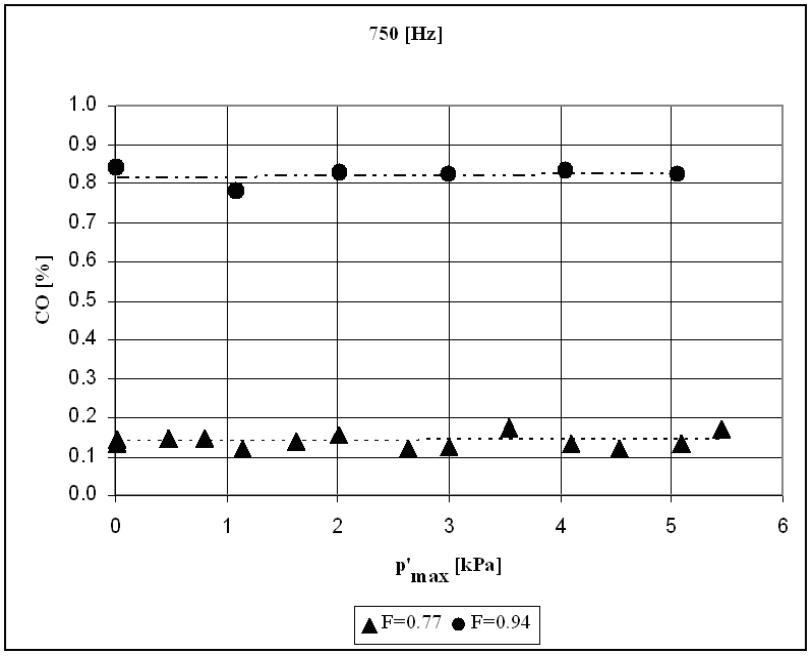

Figure 9. CO emission versus p'_{max} , for 750 Hz and equivalence ratios (F) of 0.77 and 0.94.

Generalizing the results for NO_x, initially the excitations presence increases the pollutant emission. However, when theoretically the maximum acoustic velocity overcomes the flow average velocity, the NO_x emission reduces. This behavior has been reported in the literature for fuel gas pulsating combustion; for example, the work of Ferreira et al. (2005) for flames predominantly diffusive of liquefied petroleum gas. Therefore, the same tendency happens for the pulsating combustion of well atomized liquid fuels.

For practical systems that use liquid fuels, the acoustic excitation is a promissory technology to conciliate NO_x emissions with partial oxidation pollutants. Some cases in the present worked showed that CO and UHC emissions reduced drastically with the presence of the acoustic excitation in 264 Hz, and the NO_x had the same emission of without excitation. Following the observed tendency, if superior amplitudes had been applied, which was not possible in the experimental setup described here, the NO_x could be also reduced. However, the large fluctuations of flow displacement can generate problems of spray flame stabilization, and this implication must be subject of future works.

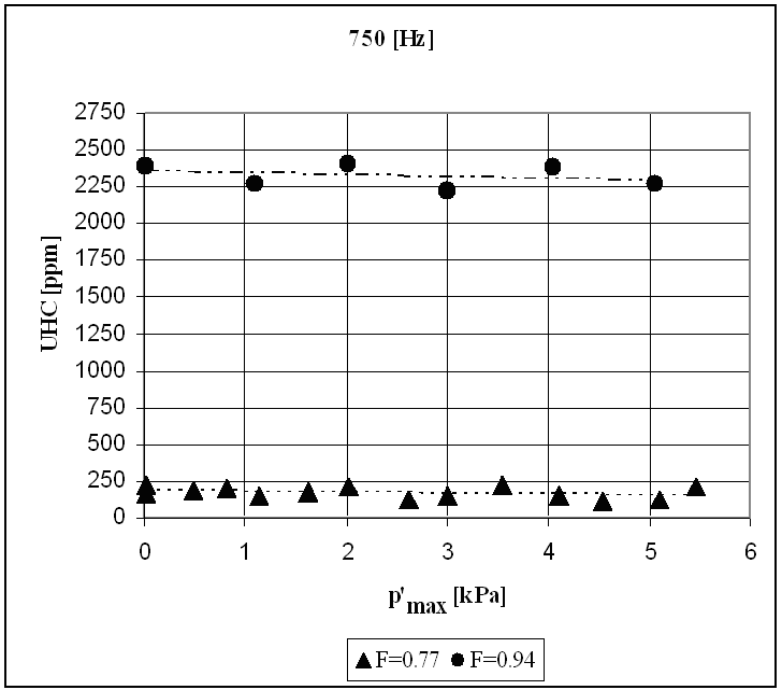

Figure 10. UHC emission versus p'_{max} , for 750 Hz and equivalence ratios (F) of 0.77 and 0.94.

REFERENCES

Dattarajan**,** S., Lutomirski A., Lobbia R. Acoustic excitation of droplet combustion in microgravity and normal gravity. Combustion and Flame 144 (1-2): 299-317, 2006.

Dubey, R.K**.**, Black. D.L., McQuay, M.Q., The effect of acoustics on an ethanol spray flame in a propane-fired pulse combustor, Combustion and Flame, 110 (1-2): 25-38,1997.

Ferreira, D.S.; Lacava, P.T.; Ferreira, M.A.; Carvalho, J.A., The Influence of the Flame Structure on the Combustion Oscillations in a Cylindrical Chamber. Proceedings of the 12th AIAA/CEAS Aeroacoustics Conference/27th AIAA Aeroacoustics Conference, 10 pages, 2006.

Ferreira, D.S.; Lacava, P.T.; Carvalho, J.A., Ferreira, M.A., Experimental Aspects of Partially Premixed Pulsating Combustion, Proceedings of the 3rd International Energy Conversion Engineering Conference, San Francisco, USA, 10 pages, 2005.

Glarborg, P., "NO_x Chemistry in Pulse Combustion", Workshop in Pulsating Combustion and its Applications, Keynote Lecture C, Lund Institute of Technology, Sweden, August 2-5, 1993.

Keller, J.O., Bramlette, T.T., Barr, P.K., Alvarez, J., paper presented at the 1993 Spring Meeting of the Western States Section/The Combustion Institute, Utah, 1993.

Lacava, P.T., Pimenta, A.P., Bastos Netto, D.,Design Procedure and Experimental Evaluation of Pressure-Swirl Atomizers. In: 24th International Congress of the Aeronautical Sciences, Yokohama, 2004.

Libby, P.A. and Williams, F.A., Turbulent Reacting Flows, Academic Press, New York, 1994.

Rocha A. M. Carvalho Jr. J. A. Lacava P. T. Application of Pulsating Combustion in the Delft Jet Diffusion Flame Burner. Brandbrief TU Delft. 13(1): p. 22-25, 2006.

Zinn, B.T., Pulsanting combustion. In: Advanced Combustion Methods, ed. F.J.Weinberg, Academic Press, pp. 113-181, 1986.

Zinn, B.T., "Pulse combustion applications: past, present and future", in Unsteady Applied Sciences-Vol. 306., Klumer Academic Publishers, pp.113 – 137, 1996.

Yoshida H. Koda M. Ooishi Y. Kobayashi K.P. Saito M., Super-Mixing Combustion Enhanced by Resonance between Micro-shear Layer and Acoustic Excitation. International Journal of Heat and Fluid Flow, 22:372-379, 2001